

## Binormal Model of Ensemble Partial Cloudiness

W. S. LEWELLEN AND S. YOH

*Department of Physics and Atmospheric Science, Drexel University, Philadelphia, Pennsylvania*

(Manuscript received 15 October 1991, in final form 2 July 1992)

### ABSTRACT

A new formulation of partial cloudiness parameterization has been introduced that agrees with that for a random model in one limit and approaches the simple updraft/downdraft model of larger-scale models in the limit of very highly skewed flow. Each of the conserved variables, liquid potential temperature and total humidity, along with the vertical velocity, are assumed to have probability distributions that may be parameterized as combinations of two multivariate normal distributions. This allows the skewness of the variables to be controlled by the bias between the means of the two normals and their relative fractions. It also provides a smooth transition between the normal distribution and the two limiting delta function distribution of the updraft/downdraft model. Comparisons with large-eddy-simulation data show this new model to be valid over a much wider range of conditions than the single normal distribution.

When a simple cloud-top entrainment instability (CTEI) analysis is made using the new binormal model, variations in the dynamic characteristics, here represented by the skewness in the extended liquid water function,  $s$ , are found to mask the variation with respect to the ratio in the thermodynamic jump conditions. This helps to explain the observed poor correlation of empirical cloud fraction with this jump condition. On the other hand, the analysis suggests that the ratio of the mean value of the extended liquid water variable,  $s$ , to the square root of its variance, may be expected to show a much better correlation with the empirical cloud fraction.

### 1. Introduction

It has long been recognized that turbulent fluctuations in moisture and temperature lead to cloud inhomogeneities on a wide range of scales, and attempts have been made to allow for averaging over these in elemental grid volumes in some numerical models. The ensemble averaging used in such cloudiness parameterizations has been reviewed by Cotton and Anthes (1989). Schemes have been proposed by Sommeria and Deardorff (1977), Mellor (1977), Manton and Cotton (1977), Oliver et al. (1978), and Bougeault (1981). None of these attempt to model aerosol growth dynamics in an inhomogeneous two-phase environment. Rather, they assume that complete knowledge of moisture, temperature, and pressure fluctuations would allow determination of the liquid water properties; that is, that there are always ample nucleation sites, that condensation dynamics are sufficiently fast, and that no local regions of significantly supersaturated vapor will occur.

Both Sommeria and Deardorff (1977), and Mellor (1977) assumed a Gaussian probability distribution for fluctuations in two conservative variables, total moisture and liquid potential temperature. This allowed the liquid water properties to be determined as

a function of the mean and variance of these two variables. Bougeault (1981) showed that the probability distributions of the two conserved variables become more skewed when the cloud fraction is small and produced LES numerical results that agreed better with a positively skewed exponential distribution. Randall (1987) demonstrated that when the cloud fraction is small, the phenomenological updraft/downdraft model commonly used for tropospheric cumulus parameterization leads to buoyancy fluxes in marked conflict with the partial cloudiness Sommeria-Deardorff-Mellor (SDM) formulation. In this limit the clouds are separated by regions of slowly subsiding air, so that there is a very strong correlation between the narrow updrafts and the clouds. This tends to produce a very skewed distribution of temperature and humidity fluctuations, in contrast to the Gaussian assumption.

In the present paper, we will present an extension of the SDM formulation that allows it to approach Randall's updraft/downdraft model in the limit of very highly skewed cloud distributions. Rather than use the Gamma distribution suggested by Bougeault (1982), we choose a binormal distribution, which is the superposition of two normal distributions.

The SDM ensemble model was used to investigate fractional cloudiness at the top of the marine boundary layer by Lewellen et al. (1990). An important parameter in the thermodynamic stability of the cloud-top inversion is the ratio of the jump in humidity to the jump in temperature across the capping inversion as

---

*Corresponding author address:* W. S. Lewellen, Mechanical and Aerospace Engineering, West Virginia University, Morgantown, WV 26506-6101.

predicted by the cloud-top entrainment instability (CTEI) analyses of Randall (1980) and Deardorff (1980). However, observations have shown that the cloud top may be unstable according to this CTEI criterion, without the cloud deck greatly reducing its fractional coverage (e.g., Hanson 1984; Albrecht et al. 1985; Nicholls and Turton 1986; Kuo and Schubert 1988; Weaver and Pearson 1991). Internal mixing dynamics appear to force strong modifications to the simple criterion. Attempts to include mixing effects in the CTEI analysis have been made by Siems et al. (1990), MacVean and Mason (1990), and Betts and Boers (1990). However, none of these have been completely successful, as pointed out by Albrecht (1991), who concludes that boundary-layer dynamics must be considered to fully parameterize the fractional cloudiness. We will use the new binormal partial cloudiness model to again investigate this controversy.

**2. Review of ensemble partial cloudiness**

We are interested in a cloud ensemble representation that can be used for subgrid parameterizations in numerical cloud models. This implies at least a spatial-average ensemble, but we believe it is more appropriate to consider a true Reynolds average over all the possible subgrid flow combinations that are compatible with the resolved scale variable information. We assume the ensemble average is defined by knowing at least two moments of the primary variables. The new model to be provided in the next section will require information on three moments. The intent is to provide a sufficiently general representation that it can be used for a wide range of length scales, from 50 m to 50 km.

We start from the basic SDM formulation and extend it by providing for the possibility of incorporating skewed distributions. It is convenient to define an extended liquid water specific humidity,  $s$ , which is equal to the liquid water specific humidity when it is positive, but can also be negative. Following Sommeria and Deardorff (1977) and Mellor (1977), we define  $s$  in terms of the approximately conserved liquid water potential temperature,  $\theta_l$ , and total water mixing ratio,  $h$ , as

$$s = (h - h_{sl}) / (1 + \alpha L / c_p), \tag{1}$$

where  $h_{sl}$  is the saturation specific humidity at a given value of  $T_l = \theta_l T / \theta$ ,  $\alpha$  is the slope of the saturated humidity with respect to temperature at constant  $T_l$  [ $\alpha = 0.622 L h_{sl} / (R_d T_l^2)$ ],  $L$  is the latent heat of vaporization;  $R_d$  the gas constant for dry air,  $c_p$  the specific heat of the mixture at constant pressure,  $T$  the temperature, and  $\theta$  is the potential temperature.

If we assume a normal distribution for the fluctuations in  $s$ , then the cloud fraction  $\bar{r}$ , average liquid water content  $\bar{h}_l$ , and liquid water variance  $\bar{h}_l'^2$  may all be obtained by integrals over this probability distribution and expressed in terms of the first two mo-

ments of the total water mixing ratio,  $h$ , and the liquid potential temperature  $\theta_l$ . This leads to the following expressions for

cloud cover:

$$\bar{r} = \frac{1}{2} [1 + \text{erf}(\zeta / \sqrt{2})]; \tag{2}$$

liquid water mixing ratio:

$$\bar{h}_l = \sigma_s (\zeta \bar{r} + e^{(\zeta^2/2)/\sqrt{2\pi}}); \tag{3}$$

and liquid water variance:

$$\bar{h}_l'^2 = \sigma_s^2 (\bar{r} - (\bar{h}_l / \sigma_s)^2 + \zeta \bar{h}_l / \sigma_s), \tag{4}$$

with

$$\zeta = \mu / \sigma_s \tag{5}$$

and

$$\mu = (\bar{h} - h_s(\bar{T}_l)) / (1 + \alpha L / c_p), \tag{6}$$

$$\sigma_s = (\bar{h}'^2 - 2\alpha_1 \bar{\theta}_l' \bar{h}' + \alpha_1^2 \bar{\theta}_l'^2)^{1/2} / (1 + \alpha L / c_p). \tag{7}$$

In this last expression  $\alpha_1 = \alpha \theta / T$ . Equations (2) and (3) are the same as the expressions given by Sommeria and Deardorff (1977) and Mellor (1977), except Mellor leaves out the square root sign in the  $2\pi$  factor in Eq. (3). Sommeria and Deardorff do not include an expression for liquid water variance, and Mellor's expression, even in his corrigendum (Mellor 1977), does not agree with Eq. (4). Equation (4) does almost agree with Chen's (1991) expression for liquid water variance; that is, it agrees if the sigma in his first term is squared to make his equation dimensionally correct.

In this representation, the skewness in the actual liquid water also depends on  $\zeta$ . Lewellen et al. (1990) argued that additional skewness could be introduced into the distributions by assuming  $\sigma_s$  is larger than that given in Eq. (3); that is, by assuming that the moist tail of the  $(h' - \alpha_1 \theta_l')$  distribution is larger than what would be supported by the total variance in this normal distribution of the extended liquid water. Bougeault's (1981) numerical data for conditions of approximately 10% cloudiness shows the variance in liquid water to be much larger than that implied by Eqs. (2)–(6). Later, Bougeault (1982) proposed a Gamma probability distribution with an added skewness parameter, which would be available to the third-order closure model he was using. We propose to get the same type of effect, by allowing each of the conserved variables,  $\theta_l$  and  $h$ , to have probability distributions that may be parameterized as combinations of two normal distributions. This binormal distribution allows the skewness of the variables to be controlled by the bias between the means of the two normals and their relative fractions. More importantly, it provides a smooth transition between the normal distribution likely to be appropriate for averages over scales of a few meters and the limiting two delta function distribution of the up-

draft/downdraft model expected to be more appropriate for averages over very large scales.

### 3. A new binormal model

#### a. Moment relationships

If the primary variables are composed of binormal distributions so that

$$f(h, \theta_i, w) = \delta f_1 + (1 - \delta) f_2, \quad (8)$$

where  $f_1$  and  $f_2$  are multivariate normal distributions of  $h$ ,  $\theta_i$ , and  $w$ , then  $f(s, w)$  can also be written as a similar combination distribution, with  $s$  defined in Eq. (1) and its fluctuations approximated as a linear combination of  $h'$  and  $\theta'_i$ :

$$s' = (h' - \alpha_i \theta'_i) / (1 + \alpha L / c_p). \quad (9)$$

The first three moments of the probability distributions of any variable represented as a binormal can then be related to the parameters that make up the two normal components by the following set of equations:

$$\mu = \delta \mu_1 + (1 - \delta) \mu_2, \quad (10)$$

$$\sigma^2 = \delta(\mu_1^2 + \sigma_1^2) + (1 - \delta)(\mu_2^2 + \sigma_2^2) - \mu^2, \quad (11)$$

$$sk\sigma^3 = \delta(\mu_1^3 + 3\mu_1\sigma_1^2) + (1 - \delta)(\mu_2^3 + 3\mu_2\sigma_2^2) - \mu^3 - 3\mu\sigma^2. \quad (12)$$

The correlation between any two variables denoted by the subscripts  $i$  and  $j$  is related to the individual correlations of the normal components by

$$cr_{ij}\sigma_i\sigma_j = \delta(\mu_{i1}\mu_{j1} + cr_{ij1}\sigma_{i1}\sigma_{j1}) + (1 - \delta)(\mu_{i2}\mu_{j2} + cr_{ij2}\sigma_{i2}\sigma_{j2}) - \mu_i\mu_j. \quad (13)$$

If  $\sigma_1$  and  $\sigma_2$  were set to zero this would reduce to the delta function relations of the updraft/downdraft model, while if  $\mu_1 = \mu_2$  and  $\sigma_1 = \sigma_2$ , the skewness is zero and the normal distribution again prevails.

At this point, we have introduced more parameters than we can conveniently determine in a general model, so some simplifying assumptions are desired. Three such assumptions are

- 1) The  $\delta$  has the same value for all variables;
- 2) The probability distribution function (pdf) for each variable is to be describable by no more than three parameters;
- 3) The correlation between each pair of variables is to add no more than one additional parameter.

This set of assumptions, together with the moment Eqs. (10)–(13), leads us to the following nonunique parameterization:

$$\mu_{1i} = \mu_i - B_i(1 - \delta), \quad (14)$$

$$\mu_{2i} = \mu_i + B_i\delta, \quad (15)$$

$$\sigma_{1i}^2 = \sigma_i^2 - B_i^2(1 - \delta)(1 + \delta + \delta^2)/(3\delta), \quad (16)$$

$$\sigma_{2i}^2 = \sigma_i^2 + B_i^2(1 - \delta)^2/3, \quad (17)$$

$$sk_i\sigma_i^3 = B_i^3(1 - \delta), \quad (18)$$

$$cr_{ij}\sigma_i\sigma_j = B_iB_j\delta(1 - \delta) + \delta cr_{ij1}\sigma_{i1}\sigma_{j1} + (1 - \delta)cr_{ij2}\sigma_{i2}\sigma_{j2}, \quad (19)$$

$$cr_{ij1} = cr_{ij2}. \quad (20)$$

By subtracting Eq. (14) from Eq. (15), it can be seen that the new variable  $B_i$  is the bias between the means of the two separate normal components. We also restrict  $\delta$  to range between 0.75 and 1 so that the subscript 1 always represents the larger fraction component. The lower limit of 0.75 has the feature that for given skewness of any two variables, this will lead to the maximum value of the large eddy contribution to the correlation between those two variables according to Eqs. (18) and (19). If we were to restrict  $\delta$  to be equal to 0.75 always, then Eq. (16) could lead to imaginary values of  $\sigma_{1i}$  when  $sk_i$  is sufficiently large. More importantly, it would not allow the representation of either very narrow updrafts or downdrafts. This can be accomplished by allowing  $\delta$  to approach 1 at large values of  $|sk_i|$  in such a way as to only let  $\sigma_{1i}$  approach 0 as  $\delta$  approaches 1. For the results presented below this was achieved by not allowing  $B_i^2/\sigma_i^2$  to exceed  $\delta^2/(1 - \delta)$ ; that is,  $\delta$  is determined by the following expression:

$$\delta = 0.75, \quad \text{if } sk_{\max} < 0.84$$

$$\delta = [sk_{\max}^2(1 - \delta)]^{(1/6)}, \quad \text{if } sk_{\max} > 0.84, \quad (21)$$

where  $sk_{\max}$  represents the skewness of the variable with the largest skewness. Equation (21) forces  $\delta$  to approach 1 as the skewness approaches plus or minus infinity. These rules allow both  $B_i$  and  $\delta$  to be uniquely determined by the skewness. This set of equations allows the representation of the pdf to be completely determined when its first three moments are known. Methods for determining the three moments, that is, closure, will be discussed further in section 3e. The precise transition point in Eq. (21) is somewhat arbitrary, and the results below are not very sensitive to this. It could provide the means of an adjustment to the model, if later, highly skewed data shows such an adjustment is desirable.

The most critical assumption of this parameterization represented by Eqs. (14)–(21) is that one value of  $\delta$  represents all the variables. In the limit of zero skewness, this parameterization returns to that of a single normal distribution with mean  $\mu_i$  and variance  $\sigma_i^2$ . In the other limit of skewness approaching infinity,  $\delta$  approaches 1, and the parameterization approaches that of the simple updraft/downdraft model, except one of the two components of the flow maintains some normal variation, rather than being represented by two delta functions.

*b. Dry convective boundary-layer limit*

According to Weil (1988), several authors (Misra 1982; Baerentsen and Berkowicz 1984; Weil et al. 1986) have found that a superposition of two Gaussian distributions can provide a good match to observations of the vertical velocity pdf in a dry convective boundary layer. The binormal distribution just described, with  $\delta = 0.75$ , and the first three moments chosen to fit the data, is compared to their data, and their analytical fit to that same data in Fig. 1. The fit resulting from our general parameterization is quite reasonable, comparable to their empirical one.

With the above confirmation of the parameterization for modest values of skewness, the intrinsic limits of a normal distribution for zero skewness, and the updraft/downdraft limit for a very highly skewed flow, we have reason to expect this parameterization to be reasonably valid for a wide variety of conditions.

*c. Binormal representation of partial cloudiness*

With the present binormal parameterization, the ensemble values of  $\bar{r}$ ,  $\bar{h}_l$ , and  $\overline{h_l^2}$ , representing partial cloudiness, may all be represented by relations of the type

$$\langle \dots \rangle = \delta \langle \dots \rangle_1 + (1 - \delta) \langle \dots \rangle_2, \quad (22)$$

where both  $\langle \dots \rangle_1$  and  $\langle \dots \rangle_2$  are determined by Eqs. (2)–(7) with the values appropriate for their individual

normal distributions. This permits  $\bar{r}$  to be uniquely determined as a function of two parameters:  $\zeta$ , the ratio of the mean value of extended liquid water to the square root of its variance, and  $sk_s$ , the skewness in the extended liquid water,

$$\bar{r}[\zeta, sk_s] = (1/2)(1 + \delta \operatorname{erf}[\zeta_1/2^{1/2}] + (1 - \delta) \operatorname{erf}[\zeta_2/2^{1/2}]). \quad (23)$$

The function  $\bar{r}[\zeta, sk_s]$  is presented in Fig. 2 for three values of skewness. It shows the expected increase in cloud fraction with skewness when the mean relative humidity is low, and the opposite when the mean saturation level is large. At a mean relative humidity of 100%,  $\zeta = 0$ , the cloud fraction varies inversely with  $sk_s$  by a little over  $\pm 10\%$  as  $sk_s$  varies  $\pm 3$ .

When appropriately normalized by the square root of the variance of  $s$ , the mean liquid water content,  $\bar{h}_l$ , and the liquid water variance,  $\overline{h_l^2}$ , can also be presented in the same manner, as exhibited in Figs. (3) and (4). The mean liquid water content is even less dependent on  $sk_s$ , except at very small values of  $\zeta$ . However, the liquid water variance is highly dependent on  $sk_s$ . At large negative values of  $sk_s$ , the principal variation in  $s$  occurs in subsaturated regions, and the ratio of the variance in liquid water to the variance in  $s$  is greatly reduced. On the other hand, when  $sk_s$  has a large positive value, relatively large values of liquid water will be found in a few localized regions.

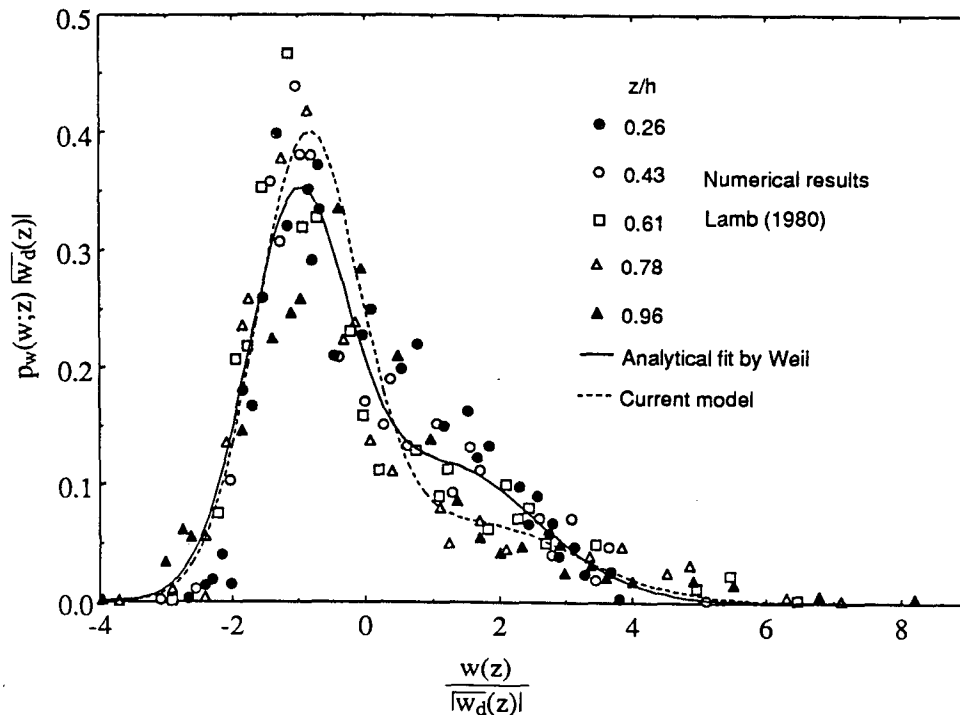


FIG. 1. Vertical velocity pdf in a convective boundary layer. Data and empirical fit taken from Weil (1988) are compared with the binormal parameterization developed in section 3.

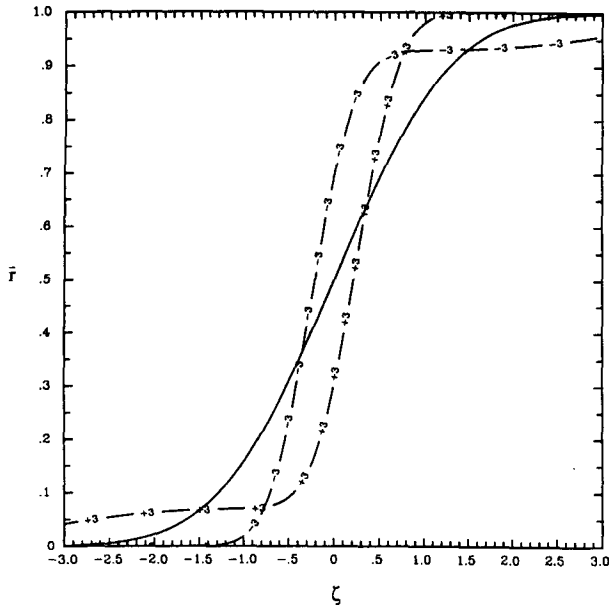


FIG. 2. Cloud fraction,  $\bar{r}$ , as a function of  $\zeta$ , the ratio of the mean value of the extended liquid water variable to the square root of its variance for three values (-3, 0, 3) of the extended liquid water skewness,  $sk_s$ .

Figures (2) and (3) are consistent with Bougeault's (1981) observation that these two quantities are not very sensitive to variations in the underlying pdf, except in the tails of the distributions.

d. Liquid water flux

The partial cloudiness parameter, which determines the feedback to the flow dynamics, is the vertical flux

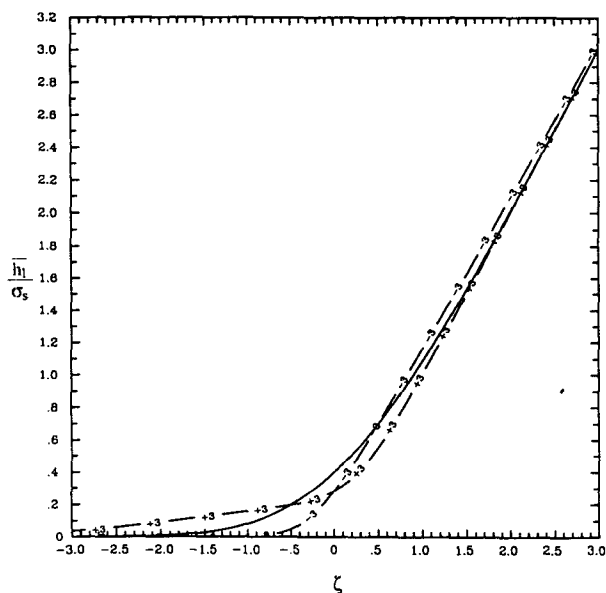


FIG. 3. Mean liquid water content as a function of  $\zeta$  for three values of  $sk_s$ .

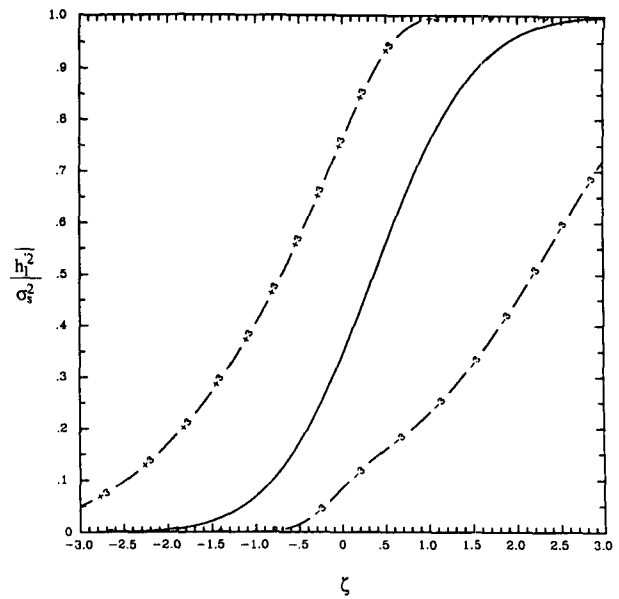


FIG. 4. Liquid water variance as a function of  $\zeta$  for three values of  $sk_s$ .

of liquid water since it is required to determine the buoyancy flux. For a reference temperature,  $T_r$ , the relation between the fluxes may be written as

$$\overline{w'\theta'_v} = \overline{w'\theta'_l} + 0.61 T_r \overline{w'h'_l} + \left( \frac{L\theta}{c_p T} - 1.61 T_r \right) \overline{w'h'_l}. \tag{24}$$

When  $w$ ,  $h$ , and  $\theta_l$  all have random normal distributions, then as argued by Sommeria and Deardorff (1977),  $\overline{w'h'_l}$  should be directly proportional to the product of the cloud fraction times its value if the volume were totally cloudy, that is,

$$\overline{w'h'_l}_{\text{normal}} = \bar{r} \overline{w's'}. \tag{25}$$

This expression is not valid for the total ensemble distribution but can still be used for the small eddy portion of the two individual normal components in our present formulation. As a result, the liquid water flux normalized by its moist value may also be presented as a function of  $\zeta$  and  $sk_s$ , but now the parameters determining the  $w$  pdf are also involved:

$$\overline{w'h'_l} = \delta \bar{r} [\zeta_1] (\mu_{1w} \mu_{1s} + cr_{sw} \sigma_{s1} \sigma_{w1}) + (1 - \delta) \bar{r} [\zeta_2] (\mu_{2w} \mu_{2s} + cr_{sw} \sigma_{s2} \sigma_{w2}). \tag{26}$$

For purposes of Fig. (5) we assume that the skewness in  $s$  and  $w$  are equal, and the small eddy correlation coefficient,  $cr_{sw}$ , between the fluctuations in these two variables is zero. The dashed line shows the variation induced by letting these small eddy correlations vary from -0.5 to 0.5. This normalized form shows relatively little variation with this correlation coefficient. There is some variation with the ratio of skewness between the two variables, which is not indicated in the

figure, but the principal message from Fig. (5) is that the liquid water flux is highly dependent on skewness. This result is consistent with Randall's (1987) observation that the highly skewed updraft/downdraft model implies quite different buoyant fluxes than the normal model of Sommeria and Deardorff (1977).

#### e. Comments on model closure

Practical use of the model provided in the previous sections requires information on the first three moments of the pdf of the primary variables and thus effectively requires some type of third-order turbulent closure model. We will not attempt to provide a new third-order closure model in this paper, but will briefly discuss three alternatives for obtaining such a model. The first possibility is to use one of the third-order closure models available in the literature (Andre et al. 1979; Bougeault 1982; and Zeman 1981). However, all of these assume that individual pdf's are quasi normal, which is incompatible with highly skewed distributions. Therefore, these types of third-order models would need to be modified before being applied to partially cloudy conditions where high values of skewness are anticipated.

We have been investigating two other alternatives for providing additional information beyond a standard second-order closure model that is required to determine the parameterization outlined in the previous sections. The first is to add dynamic equations for the bias between the means of the two normal components of each variable to the standard set of second-order closure equations. This approach utilizes the nature of the updraft/downdraft limit. It should assure compat-

ibility in this limit, and the structure of the model assures a smooth transition to the other quasi-normal limit. The major difficulty is that modeling the bias equations for this approach is roughly equivalent to a third-order closure approach in complexity.

The second alternative considered is to break the variances of the primary variables into large and small eddy contributions utilizing the split represented in Eq. (19); that is,  $B_i^2 \delta(1 - \delta)$  is the contribution from large eddies and  $\delta\sigma_{i1}^2 + (1 - \delta)\sigma_{i2}^2$  is the small eddy contribution. Separate equations for these two contributions of the variance allow both the total variance and the bias to be determined. Further, if we assume the small eddies are in equilibrium with their local environment, the equation for the small eddy variance is reduced to a diagnostic equation. The second-order closure equation for the variance may then be converted into a dynamic equation for the bias, which controls the large eddy contribution to the variance. This latter alternative allows a second-order closure model to complete the system, but it does require determining separate algorithms for the large and small eddy length scales. This alternative bears a faint resemblance to the closure recently proposed by Randall et al. (1992) in their second-order bulk boundary-layer model; that is, they would also allow the skewness to be determined by the variance equation.

Complete closure equations are not required for either of the model tests considered in the next section or in the cloud transition stability discussed in section 5. For purposes of the next section, the first three moments of the pdfs of the primary variables are assumed known from the LES data. Presentation of a new set of closure equations will be delayed until they have undergone sufficient testing for us to recommend one of the alternatives under investigation.

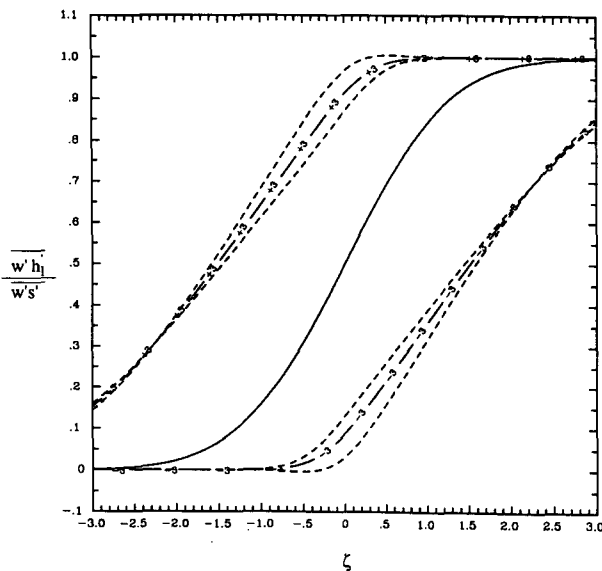


FIG. 5. Normalized vertical flux of liquid water as a function of  $\zeta$  for three values of  $sk_s$ , and the range of values of the small eddy correlations between  $s$  and  $w$  from  $-0.5$  to  $+0.5$ .

#### 4. Validation by comparison with some LES simulations

The large eddy simulation results used in this section have been previously described by Lewellen et al. (1990) and by Sykes et al. (1990), with the model more fully described by Sykes and Henn (1989). The subgrid closure utilizes a quasi-equilibrium, second-order turbulence closure scheme (Lewellen 1981) with the turbulence length scale related to the numerical grid length. The subgrid cloudiness parameterization is that given for single Gaussian pdfs. A number of simulations at different ambient conditions were used, with uniform horizontal grids of either 80 or 100 m over domains of from 4 to 8 km. Approximately 50 vertical grid points were used with minimum spacing of 25 m in the vicinity of the inversion. The turbulence is sometimes driven by the surface heat flux and sometimes by the existence of cloud-top instabilities. The simulations do not include any radiation effects.

For any height and time, a horizontal slice from the

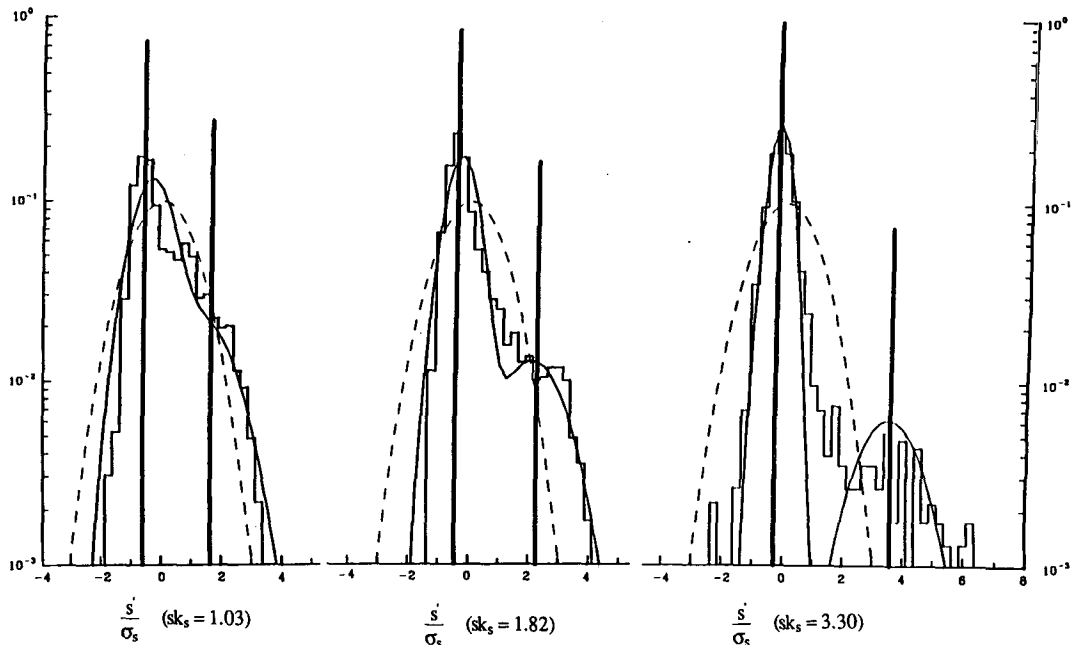


FIG. 6. Histogram of the frequency of different values of  $s$  in three example slices of the LES numerical data. Ideal normal (dashed), binormal (solid), and two delta function representations of the pdf are also shown for each given value of skewness.

LES results contains cloud characteristics at approximately 2500 points. By averaging over these slices, we can obtain numerical data to test the validity of parameterizing the partial cloudiness relations on this kilometer scale. To keep from unduly contaminating the results with the underlying subgrid parameterization, only slices where the resolved-scale, vertical liquid water flux is at least five times its subgrid contribution are used. This relatively limited sampling may be expected to produce some scatter in the results, but results were little changed by also averaging over 5 to 15 simulated minutes.

Figure 6 shows examples of histogram representations of the pdf of the extended liquid water variable,  $s$ , for three different values of skewness. The larger value shown here is close to the maximum found in this pseudo dataset. These figures also include the ideal representations of these pdfs as a normal, a binormal, and as two-delta functions. The bimodal character of the pdf shows up even at moderate values of skewness. Bougeault's (1981) histograms also show some bimodal character, although it is not included in his representation by an exponential distribution. The binormal provides a reasonable fit for all three cases. These figures, along with Fig. 1, indicate that the representation might be improved by modifying the parameterization given in Eqs. (16)–(18), so that  $\sigma_{2f}^2$  is slightly increased at moderate values of skewness; we leave this for possible later refinement.

We have compared the partial cloudiness relations developed for the binormal pdf in section 3 with the

numerical data collected from a number of simulations. The first three moments of each ensemble were computed directly from the numerical data, and the partial cloudiness relations were modeled as described. These model-derived quantities are compared with the direct numerical average of the same quantity in Figs. (7) through (10).

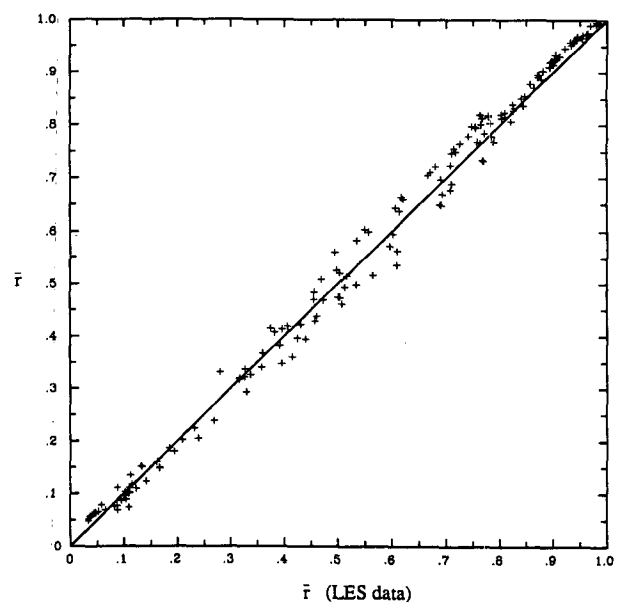


FIG. 7. Binormal model-derived cloud fraction versus direct averages of LES numerical data.

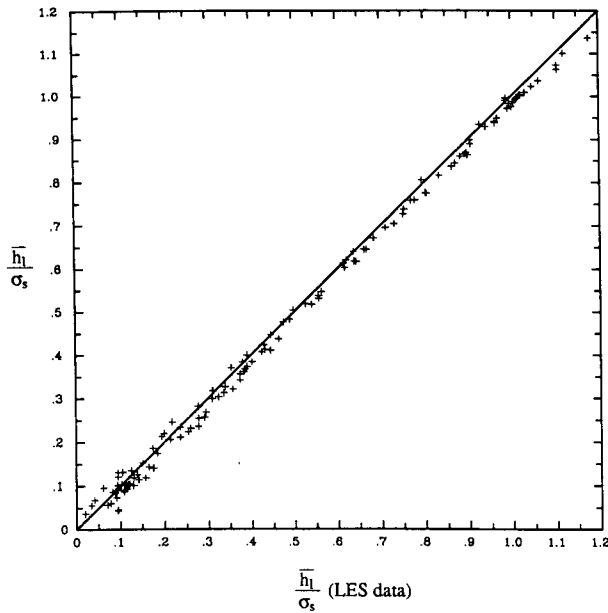


FIG. 8. Binormal model-derived cloud water content versus direct averages of the LES numerical data.

Although there is definite scatter, particularly in Figs. (9) and (10), the agreement is quite reasonable. The agreement for these last two variables is considerably better than it was for a direct comparison between the single Gaussian relationships and the data as displayed in Lewellen et al. (1990). This test demonstrates that the model validity is extended beyond the range of the single Gaussian model for boundary-layer clouds with

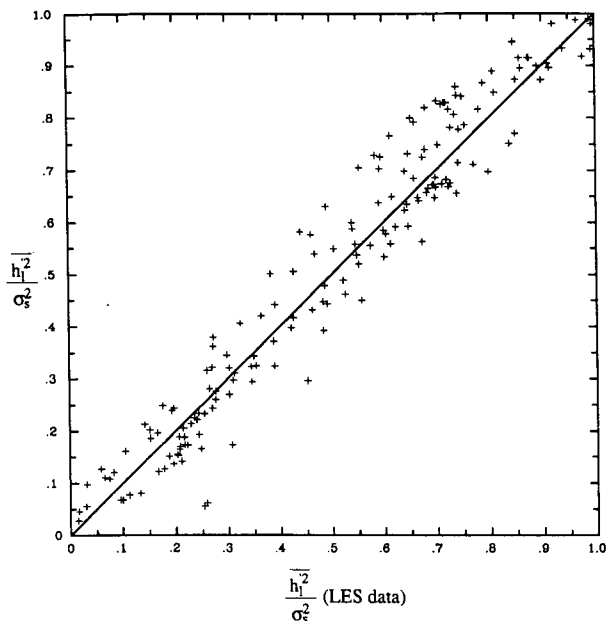


FIG. 9. Binormal model-derived liquid water variance versus direct averages of the LES numerical data.

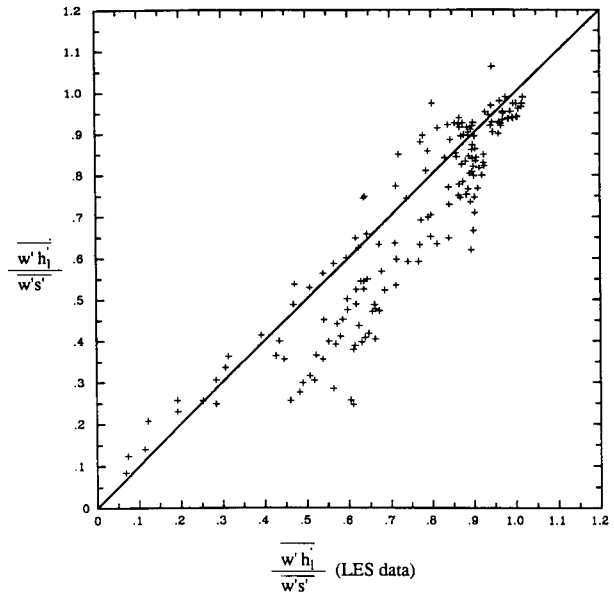


FIG. 10. Binormal model-derived vertical flux of liquid water versus direct averages of the LES numerical data.

scales up to approximately one kilometer. It still needs to be tested against scales of larger order. However, this test shows that the model should be sufficiently valid for it to be used to speculate about fractional cloudiness in the boundary layer from a one-dimensional ensemble model.

### 5. Transition cloud fraction

Cloud-top entrainment instability (CTEI) has been offered as an explanation for the breakup of boundary-layer stratus clouds (Randall 1980; and Deardorff 1980). However, observations have shown that the cloud top may be unstable according to this CTEI criterion without the cloud deck greatly reducing its fractional coverage (e.g., Hanson 1984; Albrecht et al. 1985; Nicholls and Turton 1986; Weaver and Pearson 1991). Internal mixing dynamics appear to force strong modifications to the simple stability criterion. As mentioned in the introduction, none of the attempts to include mixing effects in the CTEI analysis have been completely successful. Even without providing a dynamical simulation that requires the complete closure discussed in section 3e, we can use the basic binormal formulation proposed herein to speculate on how skewness may be expected to effect the cloud fraction that would mark the boundary between stable and unstable CTEI.

The assumption that a dynamical robust CTEI requires that the buoyant flux should increase, rather than decrease when there is an increase in entrainment, may be used to define a transition cloud fraction,  $r_{tr}$ , as was done in Lewellen et al. (1990) for the single Gaussian relationships. When the fluxes of the two



conserved variables,  $\theta_1$  and  $h$ , are approximated as an entrainment velocity,  $w_e$ , times a jump in the particular variable, Eq. (24) for the buoyancy flux may be written as

$$\overline{w'\theta'_v} = w_e \{ \Delta\theta_1 + 0.61T_r\Delta h + [(L\theta)/(c_p T) - 1.61T_r] \times \psi[\zeta, sk_s, sk_w](\Delta h - \alpha_1\Delta\theta_1) \}, \quad (27)$$

where  $\psi[\zeta, sk_s, sk_w]$  is the liquid water flux normalized by the total  $w's'$ . This function is illustrated in Fig. 5 for  $sk_s$  set equal to  $sk_w$ , which reduces it to a function of  $\zeta$  and  $sk$ . Since cloud fraction is also only a function of  $\zeta$  and  $sk_s$ , from Eq. (23) and illustrated in Fig. 2,  $\psi[\zeta, sk_s]$  may also be considered to be a function of  $\bar{r}$  and  $sk_s$ . The right-hand side of Eq. (27) may be set equal to zero to parametrically define a transition cloud fraction,  $r_{tr}$ . This allows the entrainment velocity,  $w_e$ , to cancel out, and the transition cloud fraction to be a function of the CTEI thermodynamic jump ratio,  $c_p\Delta\theta_1/L\Delta h$ , and the skewness:

$$\psi[r_{tr}, sk_s] = \frac{(c_p\Delta\theta_1/L\Delta h + 0.61c_pT_r/L)}{(\theta/T - 1.61c_pT_r/L)(1 - \alpha_1\Delta\theta_1/\Delta h)}. \quad (28)$$

Note that this analysis does not require any specific information about  $w_e$ ; we are really only assuming that the ratio of the two fluxes is proportional to the respective jump ratio of the two variables. Figure 11 is the result of parametrically allowing  $\zeta$  to vary in Eqs. (23) and (28) to obtain  $r_{tr}$  versus  $c_p\Delta\theta_1/L\Delta h$  for fixed values of skewness and the similar temperature and

pressure levels as used in the LES runs. Combinations of cloud fraction and jump ratio to the left of each line represent unstable conditions that should force the turbulence and thus the entrainment velocity to grow. Combinations to the right of the lines represent stable conditions. The transition boundaries have been drawn for the same skewness and correlation coefficients between  $s'$  and  $w'$  as given in Fig. 5. Although it only has modest variations with this correlation coefficient, it shows a very strong dependence on skewness.

Figure 11 helps to explain the observations that relatively large cloud fractions can be maintained in the face of apparent CTEI instability. If a stable cloud layer is activated by CTEI, then the induced downdrafts may be expected to lead to negative skewness in the resulting distributions of  $w'$  and  $s'$ . The result is that the transition cloud fraction stays high as skewness becomes more negative, with narrow clearing downdrafts rather than the cloud fraction decreasing along the line indicated for a zero value of skewness. When the turbulence in the boundary layer is actively driven by buoyancy flux from the surface, the resulting distributions may have positive skewness, and a sharp transition can occur at relatively high values of  $c_p\Delta\theta_1/L\Delta h$ . Thus, variations in the dynamics of the cloud layer can easily mask the expected variation with  $c_p\Delta\theta_1/L\Delta h$ . Figure 11 is compatible with Albrecht's (1991) assertion that the character of the boundary-layer dynamics is needed in addition to the thermodynamic stability of the cloud top.

A comparison of Figs. 2 and 11 suggests that the cloud fraction parameter introduced by SDM,  $\zeta$ , the ratio of the mean value of the extended liquid-water variable to the square root of its variance, may be expected to show a better correlation with empirical cloud fraction than does the cloud-top thermodynamic ratio. The skewness in  $s$  has a strong influence on the tails of the distributions in Fig. 2 but is relatively weak over the bulk of the range between 5%–95% cloud fraction.

### 6. Concluding remarks

A new formulation of a partial cloudiness parameterization has been introduced that agrees with that by Sommeria–Deardorff–Mellor (Sommeria and Deardorff 1977 and Mellor 1977) in one limit and approaches the simple updraft/downdraft model in the limit of highly skewed flow. This formulation requires information about skewness as well as the mean and variance of the primary variables. Comparisons with LES data show that if information on these three moments is available, then this model is valid over a much wider range of conditions than either of the limiting forms.

When a simple CTEI analysis is made using the new binormal model, it is seen that although  $c_p\Delta\theta_1/L\Delta h$  is one of the most important controlling factors, empirical correlations of this parameter with boundary-layer

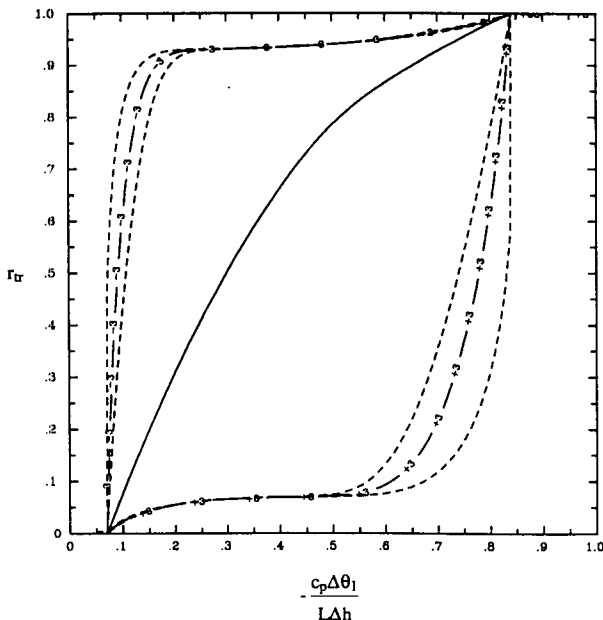


FIG. 11. Cloud fraction,  $r_{tr}$ , that marks the stability transition as a function of  $c_p\Delta\theta_1/L\Delta h$  and skewness for the same range of correlations as Fig. 5.

cloud fraction are not likely to be very good. Variations in the dynamic characteristics, here represented by the skewness in the extended liquid water function, mask the expected variation with  $c_p \Delta \theta_1 / L \Delta h$ . On the other hand, the cloud fraction parameter introduced by SDM,  $\zeta$ , may be expected to show a much better correlation with the empirical cloud fraction. It is interesting to note that over the range he tested it, Albrecht's (1981) parameterization of cloud amount also would show a strong correlation with  $\zeta$ .

The ASTEX program (Abbey et al. 1989) that has been set up to specifically study the transition from boundary-layer stratocumulus to cumulus clouds may provide a test of the parameterization proposed here. Rapid response instrumentation on an aircraft flying close to the inversion could allow a direct test of cloud fraction as a function of  $\zeta$ .

*Acknowledgments.* This work was supported by the Office of Naval Research with R. F. Abbey, Jr., technical monitor.

#### REFERENCES

- Abbey, R. F., Jr., et al., 1989: Fire Phase II Research Plan. [Available from the Fire Project Office, MS 483, NASA Langley Research Center, Hampton, VA 23665-5225.]
- Albrecht, B. A., 1981: Parameterization of trade-cumulus cloud amounts. *J. Atmos. Sci.*, **38**, 97–105.
- , 1991: Fractional cloudiness and cloud-top entrainment instability. *J. Atmos. Sci.*, **48**, 1519–1525.
- , R. Penc, and W. H. Schubert, 1985: An observational study of cloud-topped mixed layer. *J. Atmos. Sci.*, **42**, 800–822.
- Andre, J. C., G. DeMoor, P. Lacarrere, and R. DuVachat, 1979: Turbulence approximation for inhomogeneous flows. Part I: The clipping approximation. *J. Atmos. Sci.*, **33**, 476–481.
- Baerentsen, J. H., and R. Berkowicz, 1984: Monte Carlo simulation of plume dispersion in the convective boundary layer. *Atmos. Environ.*, **18**, 701–712.
- Betts, A. K., and R. Boers, 1990: A cloudiness transition in a marine boundary layer. *J. Atmos. Sci.*, **47**, 1480–1497.
- Bougeault, P., 1981: Modeling the trade-wind cumulus boundary layer. Part I: Testing the ensemble cloud relations against numerical data. *J. Atmos. Sci.*, **38**, 2414–2428.
- , 1982: Cloud-ensemble relations based on the Gamma probability distribution for the higher-order models of the planetary boundary layer. *J. Atmos. Sci.*, **39**, 2691–2700.
- Chen, J. M., 1991: Turbulent-scale condensation parameterization. *J. Atmos. Sci.*, **48**, 1510–1512.
- Cotton, W. R., and R. A. Anthes, 1989: *Storm and Cloud Dynamics*. Academic Press, 872 pp.
- Deardorff, J. W., 1980: Cloud-top entrainment instability. *J. Atmos. Sci.*, **37**, 131–147.
- Hanson, H. P., 1984: Stratocumulus instability reconsidered: A search for a physical mechanism. *Tellus*, **36A**, 355–368.
- Kuo, H.-C., and W. H. Schubert, 1988: Stability of cloud-topped boundary layers. *Quart. J. Roy. Meteor. Soc.*, **114**, 887–916.
- Lewellen, W. S., 1981: Modeling the Lowest 1 km of the Atmosphere, AGARDograph Rep. No. 267, AGARD, NATO, 81 pp. [ISBN 92-835-1407-6; available through NTIS.]
- , S. F. Parker, R. I. Sykes, S. Yoh, and D. S. Henn, 1990: Fractional cloudiness at the top of the marine boundary layer. *Proc. AMS Conf. on Cloud Physics*, San Francisco, Amer. Meteor. Soc., 101–106.
- MacVean, M. K., and P. J. Mason, 1990: Cloud-top entrainment instability through small-scale mixing and its parameterization in numerical models. *J. Atmos. Sci.*, **47**, 1012–1030.
- Manton, M. J., and W. R. Cotton, 1977: Parameterization of the atmospheric surface layer. *J. Atmos. Sci.*, **34**, 331–334.
- Mellor, G. L., 1977: The Gaussian cloud model relations. *J. Atmos. Sci.*, **34**, 356–358. [Corrigendum 1483–1484.]
- Misra, P. K., 1982: Dispersion of nonbuoyant particles inside a convective boundary layer. *Atmos. Environ.*, **16**, 239–243.
- Nicholls, S., and J. D. Turton, 1986: An observational study of the structure of stratiform cloud sheets. Part I: Structure. *Quart. J. Roy. Meteor. Soc.*, **112**, 431–460.
- Oliver, D. A., W. S. Lewellen, and G. G. Williamson, 1978: The interaction between turbulent and radiative transport in the development of fog and low-level stratus. *J. Atmos. Sci.*, **35**, 301–316.
- Randall, D. A., 1980: Conditional instability of the first kind, upside-down. *J. Atmos. Sci.*, **37**, 125–130.
- , 1987: Turbulent fluxes of liquid water and buoyancy in partly cloudy layers. *J. Atmos. Sci.*, **44**, 850–858.
- , Q. Shao, and C.-H. Moeng, 1992: A second-order bulk boundary layer model. *J. Atmos. Sci.*, **49**, 1903–1923.
- Siems, S., C. Bretherton, M. Baker, S. Shy, and R. Breidenthal, 1990: Buoyancy reversal and cloud top instability. *Quart. J. Roy. Meteor. Soc.*, **116**, 705–739.
- Sommeria, G., and J. W. Deardorff, 1977: Subgrid-scale condensation in models of nonprecipitating clouds. *J. Atmos. Sci.*, **34**, 344–355.
- Sykes, R. I., and D. S. Henn, 1989: Large-Eddy Simulation of turbulent sheared convection. *J. Atmos. Sci.*, **46**, 1106–1118.
- , W. S. Lewellen, and D. S. Henn, 1990: Numerical simulation of the boundary-layer eddy structure during the cold-air outbreak of GALE IOP-2. *Mon. Wea. Rev.*, **118**, 363–374.
- Weaver, C. J., and R. Pearson, Jr., 1991: Entrainment instability and vertical motion as causes of stratocumulus breakup. *Quart. J. Roy. Meteor. Soc.*, **116**, 1359–1388.
- Weil, J. C., 1988: Dispersion in the convective boundary layer. *Lectures on Air Pollution Modeling*, A. Venkatram and J. C. Wyngaard, Eds., Amer. Meteor. Soc., 167–228.
- , L. A. Corio, and R. P. Brower, 1986: Dispersion of buoyant plumes in the convective boundary layer. *Fifth Joint Conf. of Applications of Air Pollution Meteor.*, Boston, Amer. Meteor. Soc., 335–338.
- Zeman, O., 1981: Progress in the modeling of planetary boundary layers. *Ann. Rev. Fluid Mech.*, **13**, 253–272.